

Fabrication of Protonated $g\text{-C}_3\text{N}_4$ Nanosheets as Promising Proton Conductive Materials

Table of contents

1. Material and methods	2
2. PXRD patterns of $g\text{-C}_3\text{N}_4$ and protonated $g\text{-C}_3\text{N}_4$ nano-sheets	2
3. TEM images of protonated $g\text{-C}_3\text{N}_4$ nanosheets	3
4. FT-IR spectra of $g\text{-C}_3\text{N}_4$ and protonated $g\text{-C}_3\text{N}_4$	3
5. High resolution XPS spectra	4
6. Geometry optimization results	4
7. The TG curves	5
8. Nyquist plots of $g\text{-C}_3\text{N}_4$ at room temperature and 98% RH	5
9. Activation energies (E_a)	6

1. Material and methods

All chemicals were obtained from commercial sources and used as received without further purification. The $g\text{-C}_3\text{N}_4$ used in this work was prepared by the literature method of “*Adv. Funct. Mater.*, 2017, **27**, 1605785”. Powder X-ray diffraction data were collected using Rigaku D/MAX-rA diffractometer with Cu $K\alpha$ radiation ($\lambda = 1.5418 \text{ \AA}$). IR spectra (KBr pellets) were conducted on a Nicolet Impact 410 FTIR spectrometer in the range of $400\text{-}4000 \text{ cm}^{-1}$. Thermo-gravimetric analysis with heating from room temperature to $800 \text{ }^\circ\text{C}$ was performed using a Netzsch STA 449c analyzer in a flow of N_2 with a heating rate of $10 \text{ }^\circ\text{C min}^{-1}$. Elemental analysis (C, H, and N) was measured with a Euro EA3000 analyzer. The gas adsorption measurements were performed on ASAP 2020 apparatuses, after the sample was degassed for 4 h at $180 \text{ }^\circ\text{C}$.

2. PXRD patterns of $g\text{-C}_3\text{N}_4$ and protonated $g\text{-C}_3\text{N}_4$ nano-sheets

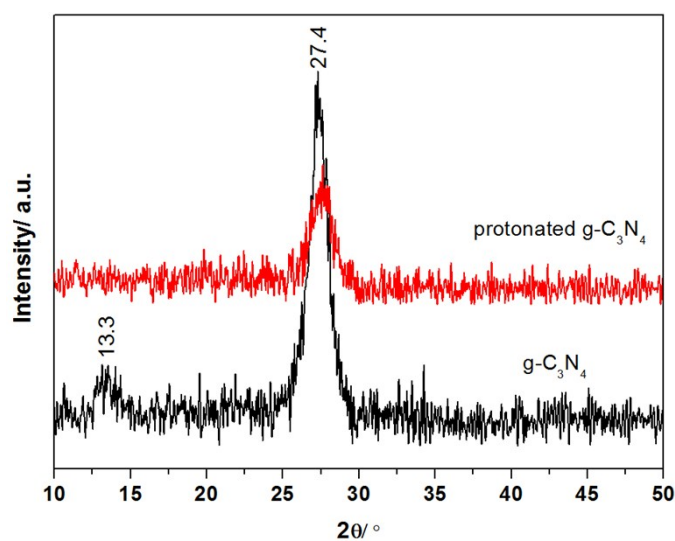


Figure S1. The PXRD patterns of $g\text{-C}_3\text{N}_4$ and protonated $g\text{-C}_3\text{N}_4$ nanosheets.

3. TEM images of protonated $g\text{-C}_3\text{N}_4$ nanosheets

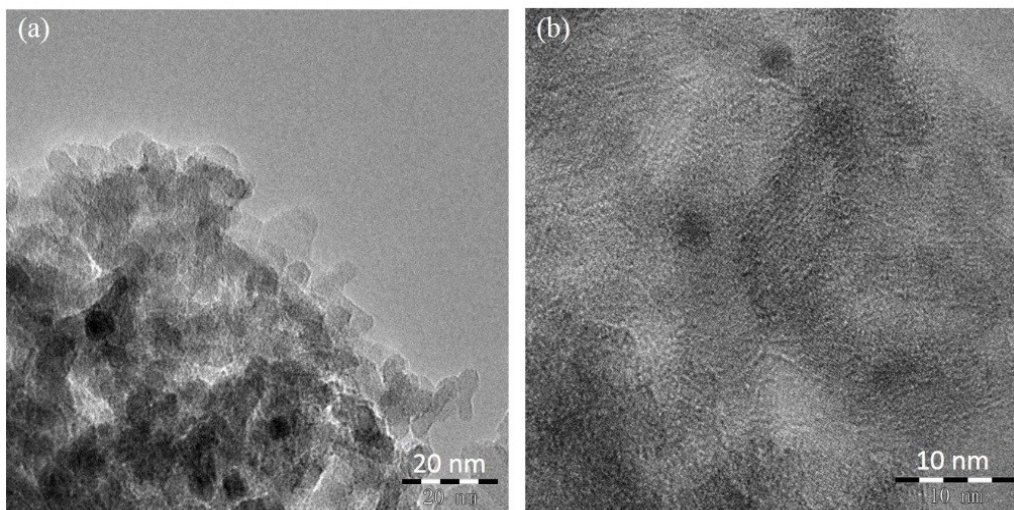


Figure S2. (a)&(b) TEM images of protonated $g\text{-C}_3\text{N}_4$ nanosheet.

4. FT-IR spectra of $g\text{-C}_3\text{N}_4$ and protonated $g\text{-C}_3\text{N}_4$

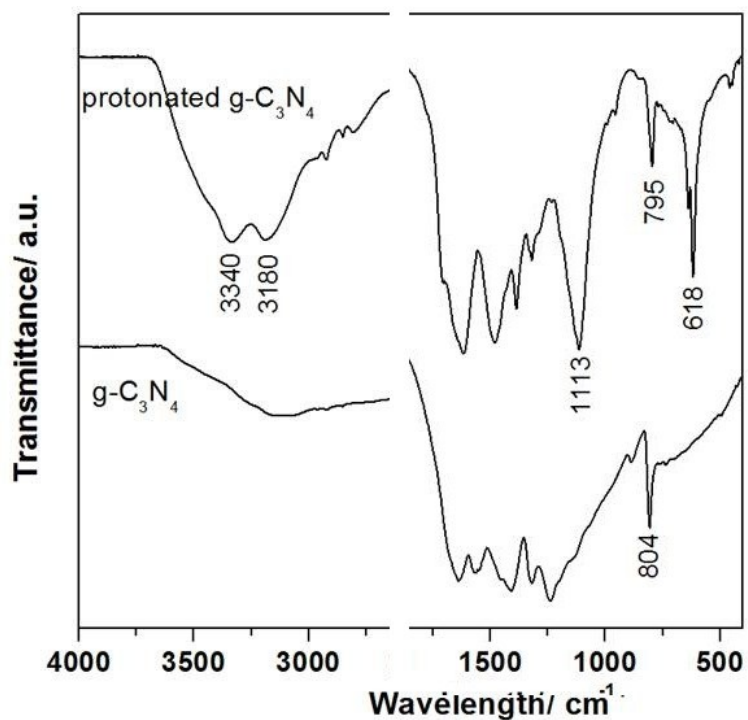


Figure S3. FT-IR spectra of $g\text{-C}_3\text{N}_4$ and protonated $g\text{-C}_3\text{N}_4$.

5. High resolution XPS spectra

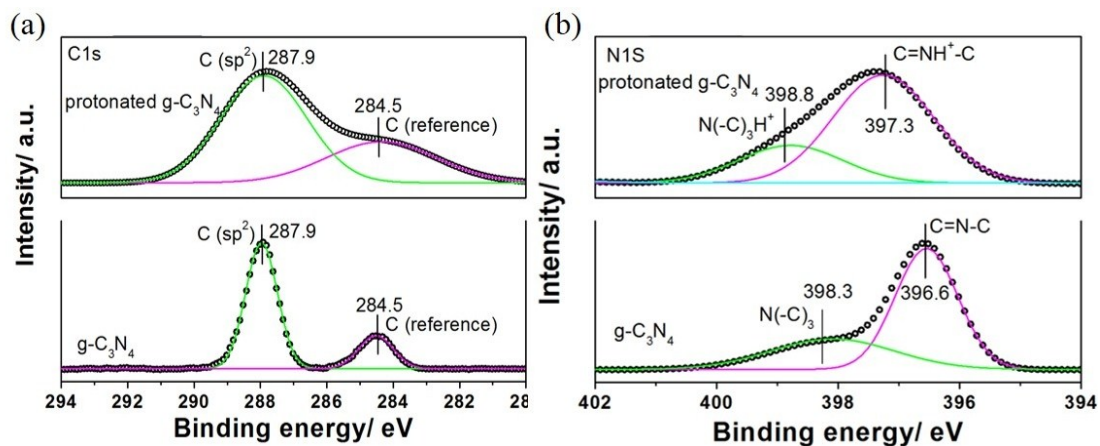


Figure S4. (a) & (b) the high resolution XPS C1s and N1s spectra of $g\text{-C}_3\text{N}_4$ and protonated $g\text{-C}_3\text{N}_4$ nanosheet, respectively.

6. Geometry optimization results

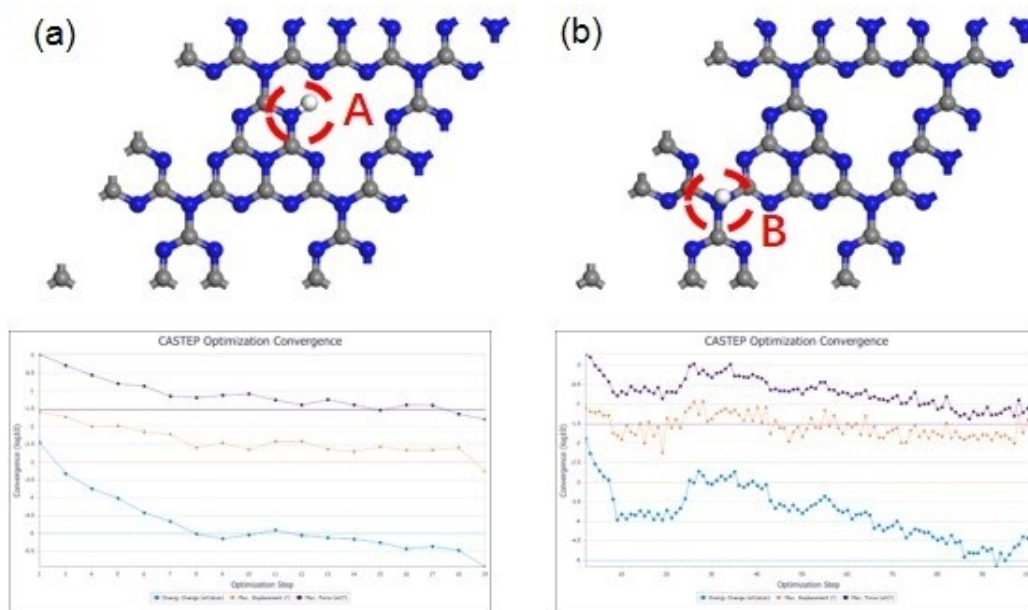


Figure S5. Geometry optimization results of protonated C_3N_4 when the protonated N was at A site (a) and B site (b).

7. The TG curves

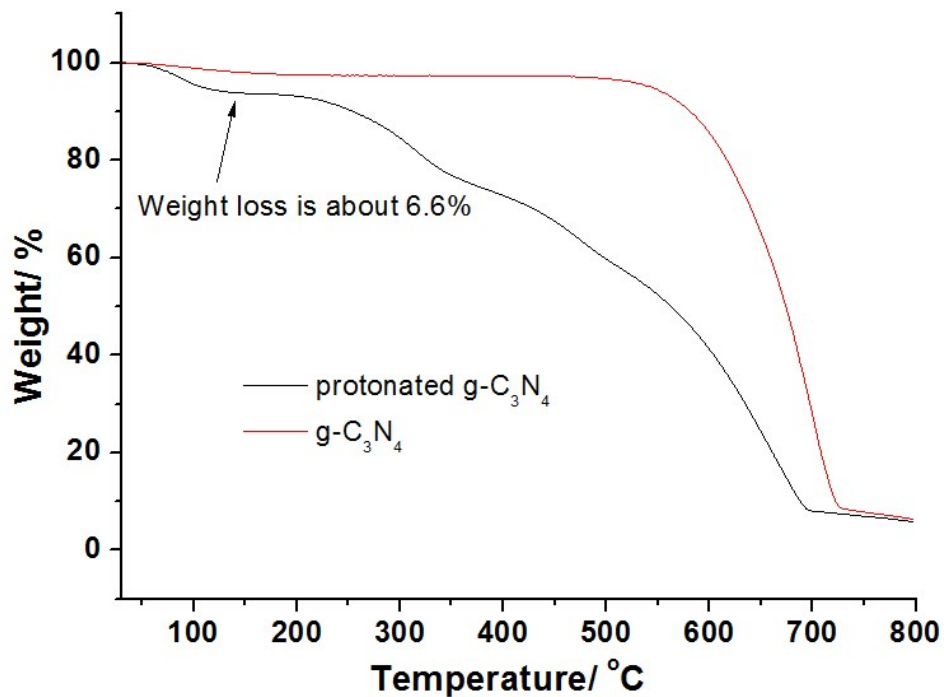


Figure S6. The TG curves of g-C₃N₄ and protonated g-C₃N₄ nanosheet.

8. Nyquist plots of g-C₃N₄ at room temperature and 98% RH

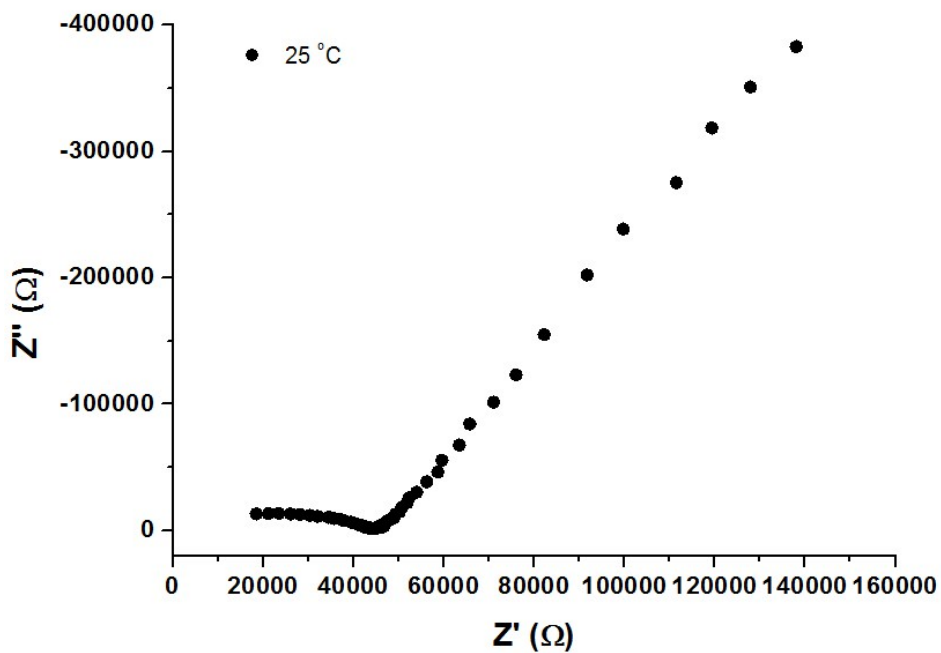


Figure S7. Nyquist plots of g-C₃N₄ under 98 % relative humidity and room temperature.

9. Activation energies (E_a)

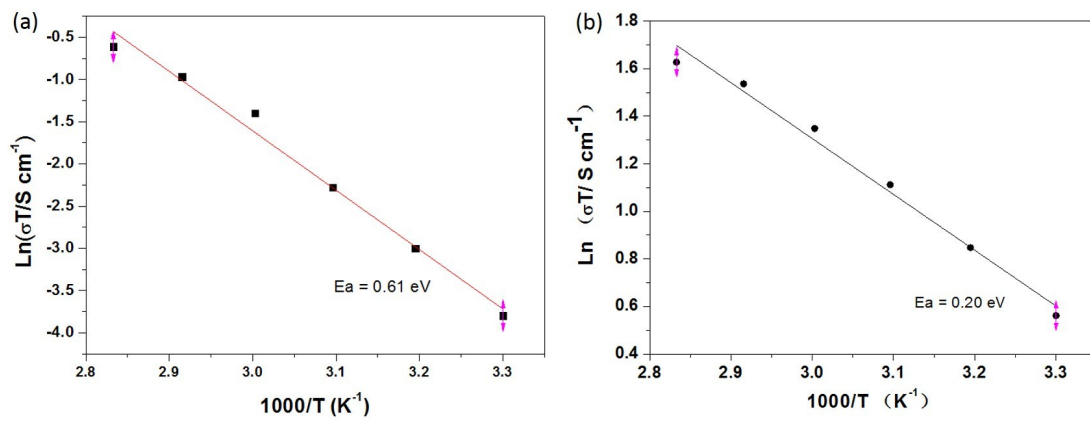


Figure S8. (a) & (b) the activation energies of $g\text{-C}_3\text{N}_4$ and protonated $g\text{-C}_3\text{N}_4$ under 98% RH from 25 to 80 °C.